Probabilistic Liquefaction Hazard Mapping

Thomas L. Holzer[1]

[1]Engineering Geologist, U.S. Geological Survey, 345 Middlefield Road, Menlo Park, CA 94025; tholzer@usgs.gov

ABSTRACT: Many investigators have applied the liquefaction potential index (LPI) to map regional liquefaction hazard. LPI, which integrates the liquefaction potential of susceptible soil elements at a specific location into a single value, has been used to assess both (1) spatial variability of liquefaction potential, and (2) liquefaction potential of surficial geologic units. A promising application to mapping has been the establishment of a median threshold LPI value at which liquefaction effects occur. This threshold when applied to complementary cumulative frequency distributions of LPI for spatially homogeneous surficial geologic units yield liquefaction probability curves for surficial geologic units that can be used for hazard mapping. Both probabilistic liquefaction scenario maps and PSHA-based liquefaction hazard maps have been produced with this approach. The scenario maps compare favorably with historical liquefaction in the mapped areas.

INTRODUCTION

Regional mapping of liquefaction hazard has evolved during the last few decades from research to regulatory endeavors (Power and Holzer, 1996). Despite this evolution, most liquefaction hazard mapping is primarily descriptive and qualitative in nature. This descriptive state-of-the-art of liquefaction hazard mapping stands in contrast with the quantitative state-of-the-art of mapping earthquake shaking hazard. Probabilistic mapping of shaking, which was originally proposed by Cornell (1968), is now firmly established and widely used in engineering practice (McGuire, 2004). In fact, confidence in the methodology has progressed to where it is now the basis in many building codes for estimating shaking hazard (BSSC, 2001; Frankel et al., 2002). The methodology is known as probabilistic seismic hazard analysis (PSHA). A comparable probabilistic framework, here referred to as probabilistic liquefaction hazard analysis (PLHA), is an important need for future liquefaction hazard mapping.

A major obstacle to the implementation of PLHA has been the absence of a widely accepted engineering demand parameter, i.e., a liquefaction intensity parameter that measures the severity of liquefaction at a site. Recently, several investigators have produced probabilistic liquefaction hazard maps for earthquake scenarios that use a parameter known as the liquefaction potential index (LPI) as an intensity parameter.

Although LPI has been widely used for seismic microzonation, the application to probabilistic mapping is new. This paper describes LPI and evaluates its potential application to probabilistic liquefaction hazard mapping.

Characterization of regional liquefaction hazard in a probabilistic framework has two important applications in addition to the informational aspect of indicating locations of significant hazard. First, as the practice of earthquake engineering transitions to performance-based design (Porter et al., 2007), characterization of hazard in a manner suitable for estimating risk is desirable. This requires that the hazard causing the risk be cast in a probabilistic framework. And second, the rapidly developing field of loss and damage estimation requires annual probabilities of hazard to compute annualized loss and damage.

LIQUEFACTION PREDICTION

Resistance of a soil to liquefaction is determined by a combination of multiple soil properties and environmental factors (Seed and Idriss, 1982). All of these properties and factors should be taken into account in an ideal evaluation of the liquefaction resistance of a soil. Because a comprehensive evaluation of soil properties and environment is neither feasible nor practical, simplified approaches have been developed. These approaches are divided here into two categories, geotechnical and geological. Although treated separately here, the approaches often are combined for regional liquefaction hazard mapping.

The most widely-used geotechnical approach is the simplified procedure (Seed and Idriss, 1971). In this procedure, two parameters are used to predict liquefaction potential: (1) a seismic demand parameter that measures the strength of the earthquake loading, and (2) a capacity parameter that measures the resistance of the soil to liquefaction. The former parameter is based on peak ground acceleration (PGA). The latter parameter is usually based on the field penetration resistance at a specific depth. For an updated and comprehensive description of the procedure, the reader is referred to Youd et al. (2001).

The simplified procedure relies on field case histories where penetration resistance was measured in soils that were inferred either to have or not to have liquefied in historical earthquakes. These penetration resistance values are compared to seismic demand at each site, and a boundary curve is drawn between the liquefied and nonliquefied case histories. The original boundary curve was deterministic and hand drawn. Statistical analyses of the case history data, however, permit points to be associated with a probability of liquefaction (Cetin et al., 2004; Juang et al., 2003; Liao et al., 1988; Moss et al., 2006; Toprak et al., 1999; Youd and Noble, 1997).

The challenge in applying the simplified procedure to regional mapping is that penetration values measure liquefaction resistance at only a specific depth in the soil layer. Values do not predict the overall liquefaction hazard at a site, i.e., the response of the entire soil column. Thus, the geotechnical approach, which is useful for engineering analysis at specific sites, must be supplemented with other parameters or considerations if it is to predict liquefaction hazard on a regional basis. Examples where this has been done include regional mapping of lateral spread hazard by Olsen et al. (2007), who relied on soil parameters identified by Youd et al. (2002), and by Mabey et al. (1993), who relied on thickness of the liquefiable layer.

The geological approach is based on observed variations in response of different geologic deposits to earthquake shaking. This variability is caused by differences in liquefaction susceptibility. These differences are attributable to both the sedimentary process responsible for deposition of each type of geologic unit and its geologic history. The geological approach was introduced by Youd and Hoose (1977), who proposed a generic classification of the liquefaction susceptibility of different deposits on the basis of their geology and age. For example, river channel deposits less than 500 years old have a very high susceptibility, whereas channel deposits of Pleistocene age (>12,000 years old) have a very low susceptibility. For application to specific areas, the geological approach is often augmented with the geotechnical approach by using penetration tests in the geologic units to develop a susceptibility ranking of the geologic units (e.g., Tinsley et al., 1985). Baise et al. (2006) recently proposed a formal process to perform this ranking if the number of penetration tests in the different geologic units is sufficient. Similarly, if locations of liquefaction during historical earthquakes in the study area are known, the liquefaction performance of a geologic unit may be included as a factor in its susceptibility ranking (e.g., Witter et al., 2006).

The geological approach is appealing for regional mapping of liquefaction hazard because of the practicality of mapping the surficial geology of large regions. This vastly increases the efficiency of the production of hazard maps. It also can improve the accuracy with which boundaries of hazard zones can be delineated because they commonly coincide with boundaries between geologic units. Thus, the challenge for regional mapping of liquefaction hazard is how to combine geotechnical assessments of liquefaction susceptibility with geology in such a manner that it permits probabilistic assessments of liquefaction hazard on a spatial basis.

LIQUEFACTION POTENTIAL INDEX

LPI has been used for several decades to map the spatial variability of liquefaction hazard. Recently several investigators have used the index to characterize the variability of the liquefaction potential of geologic deposits. For hazard mapping, the advantage of LPI over the simplified procedure is that it predicts the liquefaction potential of the entire soil column at a specific location. The simplified procedure only predicts liquefaction potential of a soil element. By combining all of the factors of safety from a boring or sounding into a single value, LPI provides a spatially distributed parameter if multiple borings or soundings are conducted in a deposit.

The liquefaction potential index was originally proposed by Iwasaki et al. (1978) to estimate the potential for liquefaction to cause foundation damage. As a historical footnote, Iwasaki et al. (1978) used the symbol I_L for LPI, but subsequently changed it to P_L (Iwasaki et al., 1982). Because of the potential for confusion with commonly used symbols for the Atterberg liquid limit (I_L) and the probability of liquefaction of a soil element (P_L), the author prefers use of LPI (Note: Yegian and Whitman (1978) also proposed a Liquefaction Potential Index that they defined as the ratio of the shear stress caused by the earthquake to the resistance of the sand to shaking. Their index did not receive widespread acceptance, and the ratio is now known as the liquefaction factor of safety.).

LPI as originally defined by Iwasaki et al. (1978) weighs factors of safety and thickness of potentially liquefiable layers according to depth. It assumes that the severity of liquefaction is proportional to:

1. cumulative thickness of the liquefied layers;
2. proximity of liquefied layers to the surface; and
3. amount by which the factor safety (*FS*) is less than 1.0, where *FS* is the ratio of soil capacity to resist liquefaction to seismic demand imposed by the earthquake.

Iwasaki et al. (1978) defined LPI as:

$$LPI = \int_0^{20m} F\, w(z)\, dz \tag{1}$$

where

$F = 1 - FS$ for $FS \leq 1$ (2a)

$F = 0$ for $FS > 1$ (2b)

$w(z) = 10 - 0.5\, z,$ where z is the depth in meters. (2c)

The weighting factor, $w(z)$, proposed by Iwasaki et al. (1978) ranges from one at the surface to zero at 20 m. F=0 above the water table.

Iwasaki et al. (1982) and Toprak and Holzer (2003) have evaluated the significance of LPI values. Both compiled case histories that compared LPI with liquefaction observations.

The evaluation by Iwasaki et al. (1982) was based on 6 historical earthquakes in Japan where liquefaction had been reported. They concluded that "severe liquefaction is likely" at sites with LPI>15 and that "severe liquefaction is not likely" at sites with LPI<5. Their categories were based on the general likelihood of liquefaction occurrence rather than the nature of the ground deformation. From Iwasaki et al. (1982, Fig. 5), one can infer that LPI>15 at 50% of the liquefaction sites and LPI<5 at more than 75% of the sites without liquefaction effects. Their evaluation relied on standard penetration tests (SPT) blow counts to compute LPI values.

Iwasaki et al. (1982) computed factors of safety with an alternative to the Seed-Idriss simplified procedure, which they referred to as "a simple analysis." Their boundary curve is determined by median grain size (d_{50}). There is no fines correction as in the Seed-Idriss simplified procedure. Their boundary curve differs from that of the simplified procedure, generally producing lower factors of safety for clean sand as d_{50} decreases (Fig. 1). For the comparison, Japanese blow counts for $(N_1)_{60}$<20 were reduced by 10% for consistency with U.S. practice (Seed et al., 1985, p. 1433).

Toprak and Holzer (2003) evaluated LPI in two contexts, frequency and nature of ground deformation. They estimated both the probability of surface manifestations of liquefaction as a function of LPI and correlated LPI with the actual nature of the surface effects. The evaluations relied on LPI values from cone penetration test (CPT) soundings at sites with surface manifestations of liquefaction during the 1989 Loma Prieta, California, earthquake. Factors of safety were computed with Robertson and Wride (1998), the CPT-based procedure recommended by Youd et al. (2001).

To evaluate frequency, Toprak and Holzer (2003) placed LPI values into bins of one LPI unit. Each LPI value was classified as to whether or not liquefaction effects

were observed near the sounding. For each bin, frequency or probability of liquefaction was computed by dividing the number of soundings where liquefaction effects were observed nearby by the total number in the bin. They concluded that "the probability of surface manifestations of liquefaction is 58 and 93%, respectively, when LPI equals or exceeds 5 and 15." Toprak and Holzer (2003) recognized a potential for sampling bias in probability estimates if subsurface exploration is conducted primarily in areas of liquefaction. To reduce the impact of sampling bias, their recommended probabilities were computed only from field studies where CPT tests had been conducted both in and out of the liquefaction areas. They described but excluded probability estimates from other case histories where exploration was conducted principally in the area affected by liquefaction.

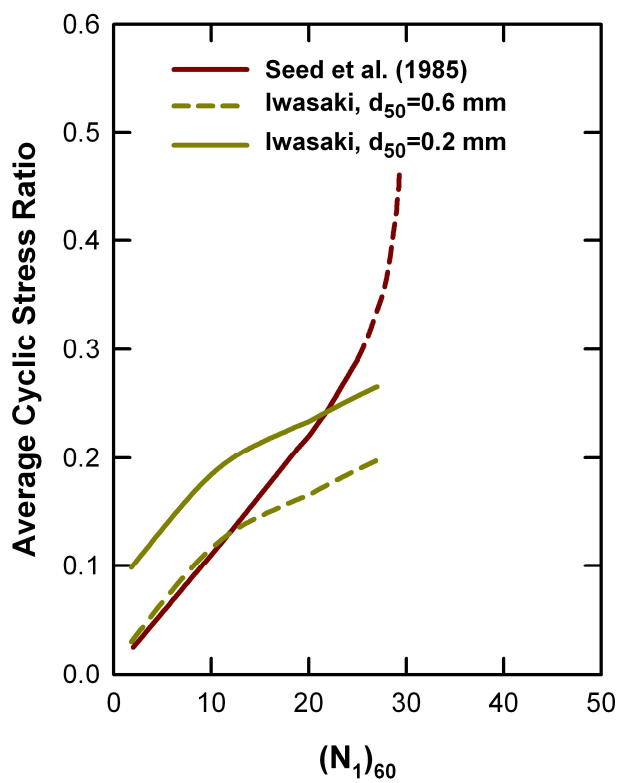

FIG. 1. Comparison of SPT boundary curves from the simplified procedure for clean sand (Seed et al., 1985) and the "simple analysis" by Iwasaki et al. (1982).

To evaluate the correlation of LPI with the severity of the surface manifestations of liquefaction, Toprak and Holzer (2003) grouped soundings into four categories based on surface effects that were observed near soundings: none, only sand boils, inchoate patterns of ground cracks, and lateral spreading. They observed that the median values of LPI were 5 and 12, respectively, in areas with sand boils and lateral spreads. Lower and upper quartiles were 3 and 10 for sand boils and 5 and 17 for lateral spreads. In addition, the threshold of LPI≥5 is supported by a field investigation of liquefaction at Oceano, California in 2003. Liquefaction caused by the M6.6 San Simeon earthquake generally occurred at locations where LPI ≥ 5 (Holzer et al., 2005a).

A few investigators have proposed modifying the severity term, *F*, in LPI (Eq. 2a). Sonmez (2003) expressed concern with the capability of LPI to identify "marginally" liquefiable soils, by which he meant soils with *FS* near one. Accordingly, Sonmez (2003) modified *F* so that it was nonzero for $0.95 \leq FS < 1.2$. This introduction of conservatism is consistent with recommendations by Seed and Idriss (1982) to adopt a *FS* between 1.25 and 1.5 to identify potentially problematic soils for engineering design. The primary impact of the modification is that it produces nonzero, but low, LPI values for soils that may warrant more detailed investigation of their liquefaction potential. This modification allowed Sonmez (2003) to subdivide the category LPI<5 by adding a hazard boundary at LPI=2.

Lee et al. (2003) proposed that *F* be replaced with the conditional probability of liquefaction derived by Juang et al. (2003). The conditional probability, $P_L = 1/[1 + (FS/0.96)^{4.5}]$, estimates the probability of liquefaction for a given soil element given a factor of safety. Lee et al. (2003) also recommended usage of the simplified procedure for the CPT as implemented by Juang et al. (2003). Lee et al. (2003) compared values computed with the redefined LPI to the occurrence of liquefaction caused by the 1999 Chi Chi earthquake and discovered it produced significantly higher values than the calibration of Iwasaki et al. (1982). This prompted them to rename their parameter the liquefaction risk index. Sonmez and Gokceoglu (2005) adopted the revision of LPI by Lee et al. (2003), but renamed it the liquefaction severity index. They also proposed a 5-category severity scale. Their parameter is not to be confused with the liquefaction severity index of Youd and Perkins (1987) that predicts ground displacement caused by lateral spreading.

To make the hazard scale of the liquefaction risk index more consistent with the LPI scale of Iwasaki et al. (1982), Li et al. (2006b) conducted a series of sensitivity tests and redefined $F = P_L - 0.35$ if $P_L \geq 0.35$ and $F = 0$ if $P_L < 0.35$. Based on this definition of *F* and the simplified procedure proposed by Idriss and Boulanger (2006), Li et al. (2006) computed revised LPI values for the 1999 Chi Chi, Taiwan, earthquake and all of the case histories reported by Toprak and Holzer (2003). They correlated these values with field-based estimates of the "probability of ground failure" and proposed a new set of liquefaction hazard categories based on these probabilities. The upper boundaries to their "risk of ground failure" categories "extremely low to none, low, medium, high, and very high" respectively, correspond to revised LPI values (and *probability of ground failure*) of 3.5 (*0.1*), 5.4 (*0.3*), 7.8 (*0.7*), 9.7 (*0.9*), and 14.1 (*1.0*). They did not recognize LPI=5, which corresponds to a probability of ground failure of 0.24, as a boundary. Their analysis of the probability of ground failure did not consider potential sampling bias. It included case histories that were excluded by Toprak and Holzer (2003) because of concerns with sampling bias. The high probabilities at intermediate LPI values might also be explained by the observation that the Youd et al. (2001) CPT-based curve is associated with a 50% probability of liquefaction (Juang et al., 2002; Toprak et al., 1999). This would yield lower LPI values when used in the traditional way as a deterministic curve.

Juang et al. (2005), following the correlation by Toprak and Holzer (2003) of LPI with type of ground deformation, proposed a damage state parameter, the damage severity index, to predict actual liquefaction-induced foundation damage. The parameter was correlated with both the revised LPI and the "probability of ground

failure" computed by Li et al. (2006b). Juang et al. (2005) advised caution in its application until the correlation could be evaluated with more case histories.

PROBABILISTIC HAZARD MAPS FOR SCENARIO EARTHQUAKES

Applications of LPI to Liquefaction Hazard Mapping

LPI has been used by many investigators to map liquefaction hazard at regional scales (Table 1). Most of the maps relied on the scale proposed by Iwasaki et al. (1982) to indicate hazard (see entries labeled "Iwasaki scale" in Table 1). With this scale, hazard boundaries are defined at LPI values of 5 and 15. Recently, three investigators have produced maps that rely on LPI to estimate the probability of liquefaction (see entries labeled "Probability" in Table 1). All of the maps in Table 1 are based on scenario earthquakes, except those by Cramer et al. (2008), which are probabilistic liquefaction hazard maps.

Table 1. Published liquefaction hazard maps based on LPI

Date	*Authors*	*Location*	*Country*	*Evaluation of LPI*
1982	Iwasaki et al.	Shizuoka Pref.	Japan	Iwasaki scale
1994	Kayabili and West	Evansville, IN	U.S.	Iwasaki scale
1998	Divakarla et al.	w. Puerto Rico	U.S.	Iwasaki scale
1998	Hosseini	Busehr	Iran	Iwasaki scale
1998	Luna and Frost	Treasure Island, CA	U.S.	Iwasaki scale
1999	Cresellani et al.	Romagna Coast	Italy	Iwasaki scale
2002	Holzer et al.	Oakland, CA	U.S.	Probability
2003	Sonmez	Inegol	Turkey	Iwasaki scale
2004	Uluzay and Kuru	Ceyhan	Turkey	Iwasaki scale
2005	Papthanassiou et al.	Lefkada	Greece	Iwasaki scale
2007	Rix and Romero-Hudock	Memphis, TN	U.S.	Probability
2007	Hayati and Andrus	Charleston, SC	U.S.	Iwasaki scale
2007	Juang and Li	Charleston, SC	U.S.	Probability*
2007	Lenz and Baise	Oakland, CA	U.S.	None
2008	Cramer et al.	Memphis, TN	U.S.	Probability

*Significant modification of definition of LPI.

Iwasaki et al. (1982) were the first to map liquefaction hazard with the "Iwasaki scale." Using their scale, they mapped areas of "no, possible and likely liquefaction" in Shizuoka Prefecture, Japan. They also relied on different types of surficial geology–"topographic zones"–to assign hazard ratings to areas. Since then, many other maps based on the "Iwasaki scale" have been published. Kayabali and West (1994) produced the first map in the United States, publishing maps of Evansville, Indiana, for two earthquake scenarios. Frost et al. (1997) were the first to implement LPI in a geographic information system and mapped liquefaction hazard on an island underlain by sandy artificial fill in San Francisco Bay, California (Luna and Frost,

1998). Maps based on the "Iwasaki scale" or modifications of it have been published for Busehr, Iran (Hosseini, 1998), western Puerto Rico (Divakarla et al., 1998),the Romagna coast, Italy (Crespanelli et al., 1999), Inegol, Turkey (Sonmez, 2003), Ceyhan Turkey (Ulusay and Kuru, 2004), Lefkada, Greece (Papathanassiou et al., 2005), and Charleston, South Carolina (Hayati and Andrus, 2007). In addition to the map by Iwasaki et al. (1982), Kayabali and West (1994), Hayati and Andrus (2007), and Lenz and Baise (2007) explicitly considered surficial geology. The other maps were based strictly on the spatial pattern of LPI. Not included here is the map by Li et al. (2006a), who mapped liquefaction probabilities in Yuanlin, Taiwan, for the 1999 Chi Chi earthquake. Their approach was partially calibrated with 1999 liquefaction effects in Yuanlin.

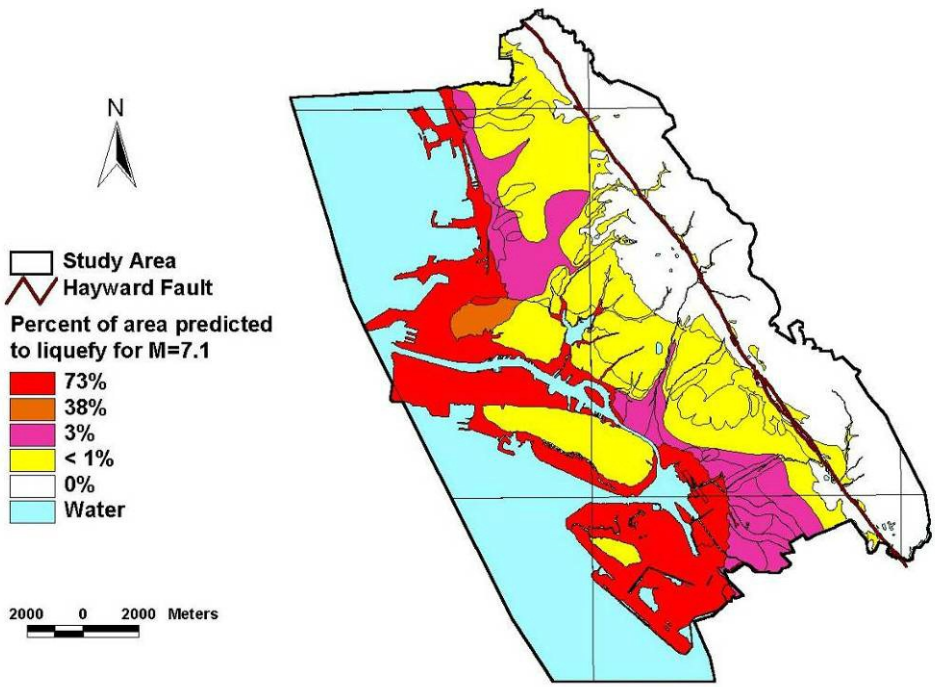

FIG. 2. Map of the greater Oakland area, California, showing percent of area expected to exhibit liquefaction during a M7.1 Hayward Fault earthquake (Holzer et al., 2002).

Mapping Liquefaction Probability

Two approaches that rely on LPI have been developed for probabilistic mapping of liquefaction. One approach relies on the LPI values of surficial geologic units (Holzer et al., 2002; 2006a). They used complementary cumulative frequency distributions of LPI of surficial geologic units to estimate probabilities of surface manifestations of liquefaction. The other approach relies directly on LPI values to estimate the spatial pattern of probabilities (Juang and Li, 2007). Both approaches use versions of the Seed-Idriss simplified procedure to compute LPI.

The liquefaction hazard map of the greater Oakland, California, area (Fig. 2) illustrates the approach proposed by Holzer et al. (2002; 2006a). It was the first regional portrayal of the probability of liquefaction based on LPI. Rix and Romero-

Hudock (2007) subsequently adopted the approach to map liquefaction hazard in Memphis, Tennessee. The greater Oakland map was based on existing surficial geologic maps and multiple seismic CPT soundings conducted in each of the surficial geologic units (Fig. 3). LPI values were computed for each sounding for scenario earthquakes on the nearby (<6 km) Hayward Fault. LPI values for each scenario were grouped by surficial geologic unit and complementary cumulative frequency distributions of the LPI values were plotted. Based on the threshold value recommended by Toprak and Holzer (2003), the frequency at LPI≥5 was used to estimate the percent area underlain by the surficial geologic unit that would exhibit surface manifestations of liquefaction. Complementary cumulative frequency values for the M7.1 (PGA=0.4 g) scenario are shown in Fig. 4. The distributions shown in Fig. 4 are called complementary cumulative frequency distributions because the frequency starts at 100% and decreases to zero with increasing LPI. Complementary cumulative frequency also is known as the frequency of exceedance.

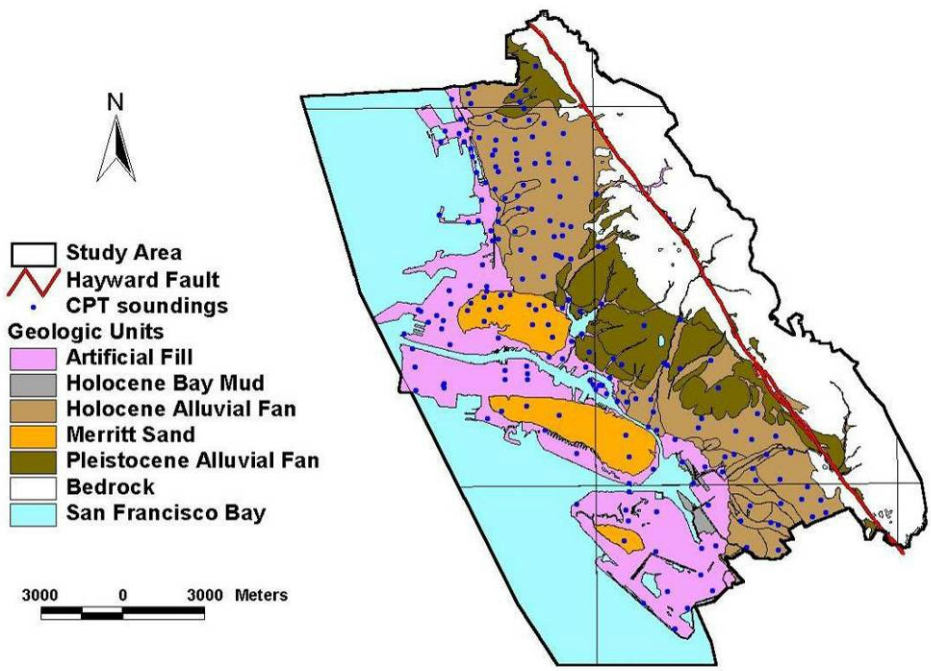

FIG. 3. Map of surficial geology of greater Oakland area, California, with CPT soundings. (Geology simplified from Helley and Graymer, 1997)

Although the complementary cumulative frequency at LPI≥5 was interpreted by Holzer (2002) to be the percent area with surface manifestations of liquefaction, it also can be interpreted as the conditional probability of liquefaction at a randomly selected location within the geologic unit given an earthquake magnitude and PGA (Holzer et al., 2006a). This assumes the unit is spatially homogeneous. The choice of interpretation of the complementary cumulative frequency is determined by the intended audience for the maps. For public officials and the general public, percent area generally may be more understandable. For engineering applications, conditional probability may be preferred.

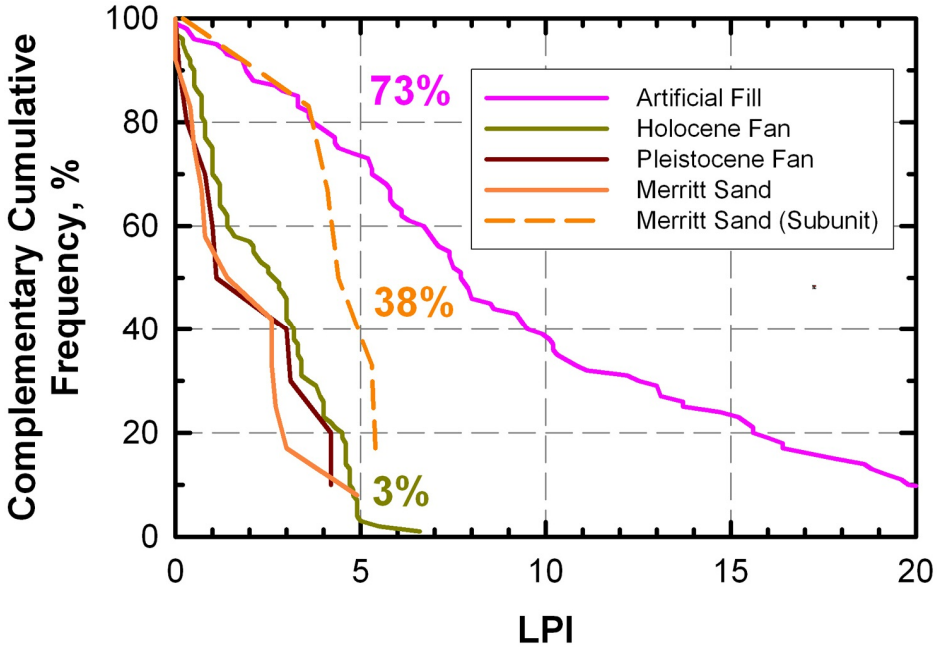

FIG. 4. Complementary cumulative frequency distributions of LPI for surficial geologic units in the greater Oakland area that were used to produce the map in Fig. 2. Earthquake scenario was a M7.1 earthquake with PGA=0.4 g. (Holzer et al., 2006a)

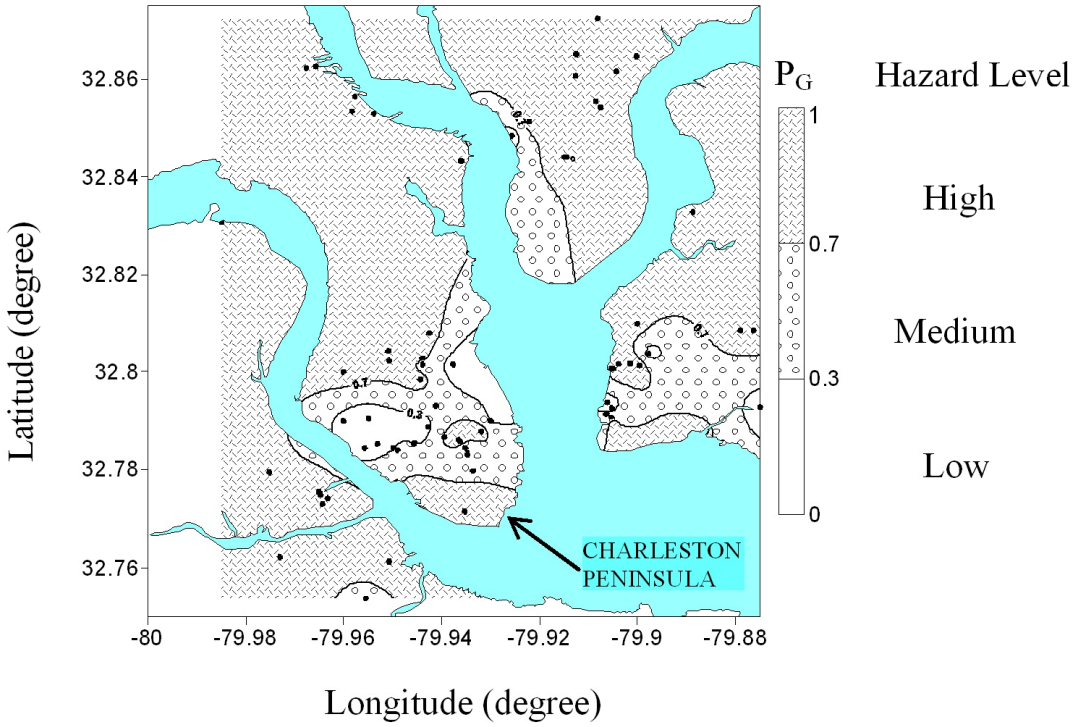

FIG. 5. Probability of liquefaction on the Charleston, South Carolina, peninsula (Juang and Li, 2007, Fig. 8)

In the approach by Juang and Li (2007), site specific LPI values are computed and used to estimate the probability of ground failure at the location of each sounding. Individual probability values are then contoured or grouped to identify areas of different liquefaction potential (Fig. 5). Surficial geologic units are only modestly considered in their approach. For their mapping of the Charleston, South Carolina, peninsula, only two geological aspects were considered. Oligocene sediment in the Cooper Group, popularly known as the Cooper marl in the Charleston area, was assumed to be nonliquefiable. If a CPT sounding was less than 20 m deep but penetrated marl, they assumed that severity term, *F*, equaled zero within the marl. They also used surficial geology as a basis for estimating site amplification factors for PGA.

Effect of Spatially Variable Ground Motion

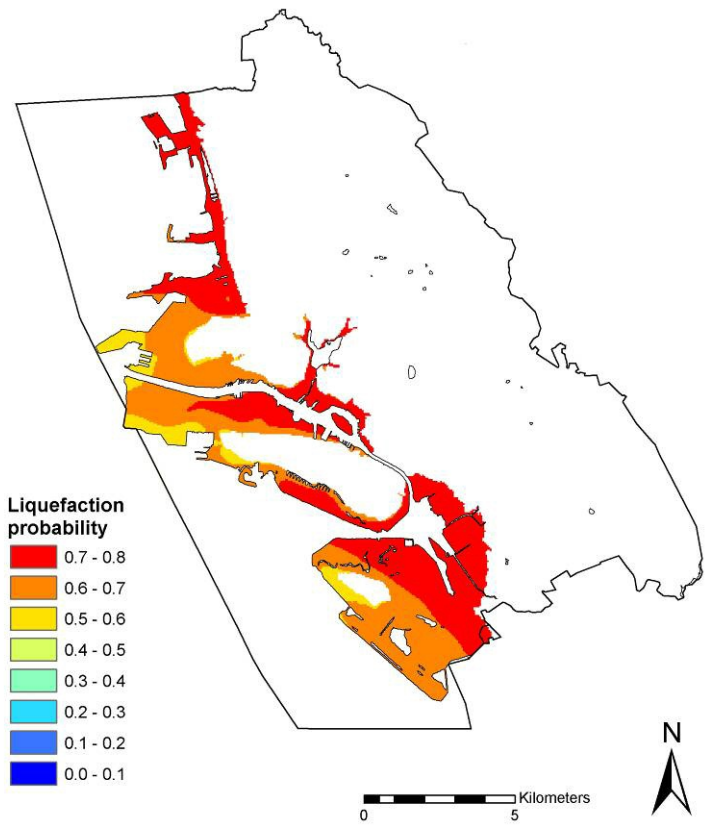

FIG. 6. Liquefaction probabilities of sandy artificial fills in the greater Oakland area based on spatially variable ground motion for M6.9 Hayward Fault earthquake. Same study area as Fig. 2. (Holzer et al., 2006b, Fig. 4)

Most of the earthquake scenarios that were used to create the maps compiled in Table 1 assume a constant PGA. This assumption can significantly oversimplify

ground shaking in areas that are prone to liquefaction. Liquefiable sediments generally occur in settings such as valleys, basins, and as fills along shorelines where thickness of underlying sediment changes laterally. These settings can cause local variations of shaking, i.e., nonuniform site response. The impact of locally variable site response on liquefaction probability is illustrated for the sandy artificial fill in the Oakland area by comparing Figs. 2 and 6. The map in Fig. 2 was based on a spatially constant PGA=0.4 g. The map in Fig. 6 is based on estimates of PGA that considered both the local 30-m, time-averaged velocity (Holzer et al., 2005b) and distance from the fault. Although the probability of liquefaction is high in both scenarios, consideration of site response introduces significant spatial variability into the liquefaction probability.

Table 2. Probabilities of surface manifestations of liquefaction for different seismic loadings of sandy artificial fills along the eastern shore of San Francisco Bay near Oakland, California (Holzer et al., 2006b).

PGA, g	***M8***	***M7.5***	***M7***	***M6.5***	***M6***	***M5.5***	***M5***
0	0	0	0	0	0	0	0
0.10	0	0	0	0	0	0	0
0.15	0.18	0.08	0.03	0	0	0	0
0.20	0.42	0.26	0.17	0.04	0	0	0
0.25	0.57	0.47	0.30	0.18	0.05	0	0
0.30	0.67	0.58	0.48	0.28	0.17	0.04	0
0.40	0.76	0.69	0.64	0.53	0.38	0.20	0.05
0.50	0.78	0.76	0.72	0.66	0.54	0.40	0.18
0.60	0.79	0.78	0.77	0.71	0.65	0.54	0.30

Predicting the probability of surface manifestations of liquefaction with spatially variable ground motions can be computationally simplified by curve fitting the relation between probability and PGA. Fig. 7b shows the relation for the Oakland artificial fills for a M6.9 earthquake, where the probability was inferred from the complementary cumulative frequency distributions of LPI (Fig. 7a). Holzer et al. (2006c) fit these data with a 3-parameter logistic equation (Fig. 7b). Rix and Romero-Hudock (2007) generalized the relation to other earthquake magnitudes by scaling the seismic demand (PGA) by the magnitude scaling factor (MSF) from the simplified procedure (Fig. 7c). For the simplified procedure as described in Youd et al. (2001), $MSF = 10^{2.24}/M^{2.56}$, where M is moment magnitude. Data points in Fig. 7c are based on the LPI≥5 threshold from complementary cumulative frequency distributions for the combinations of earthquake magnitudes and PGA compiled in Table 2. Herein for a specific surficial geologic unit, the relation between probability of surface manifestations of liquefaction and PGA scaled for magnitude will be referred to as the "liquefaction probability curve."

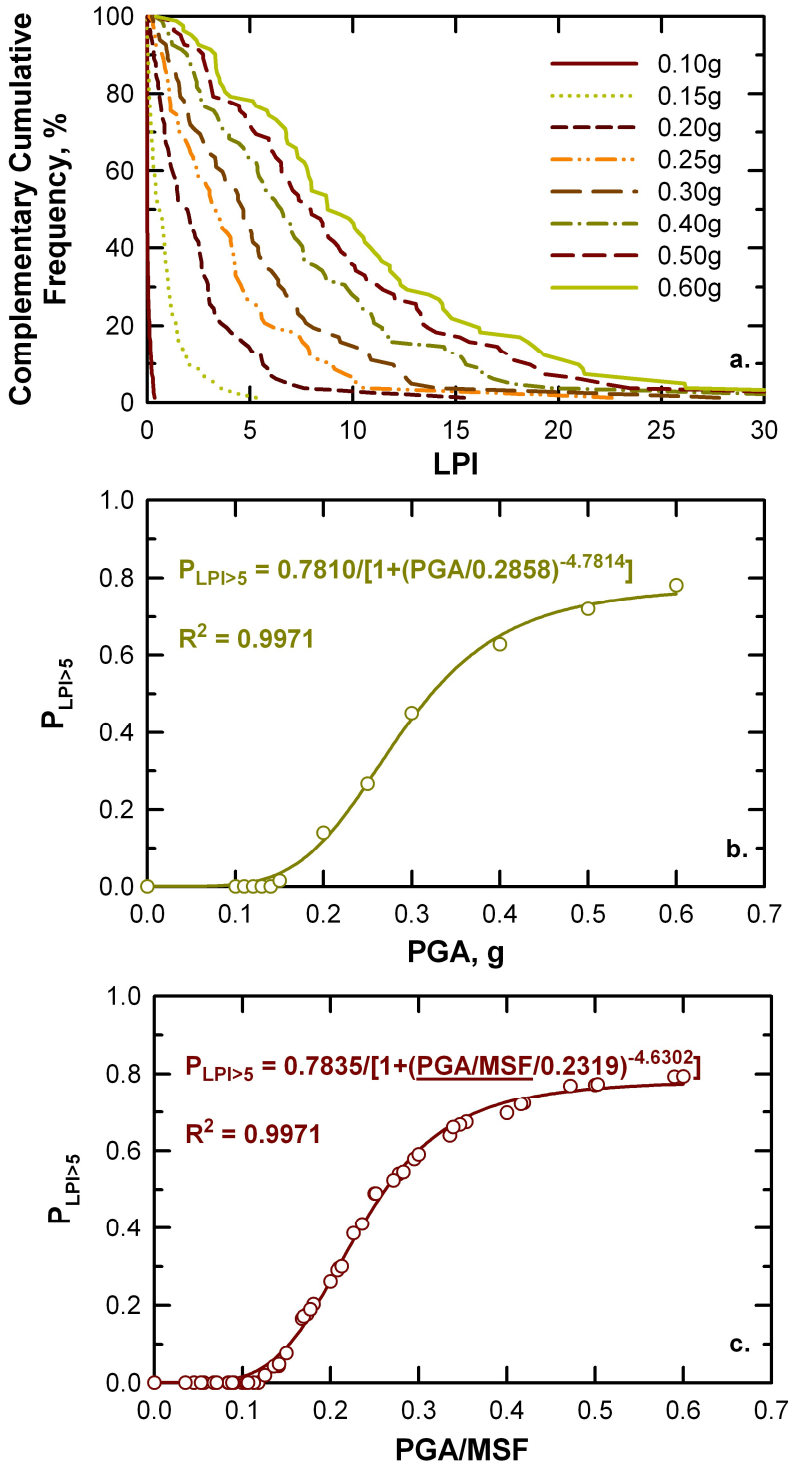

FIG. 7. Statistical properties of sandy artificial fills along shoreline of San Francisco Bay in the greater Oakland area, California. a. Complementary cumulative frequency distributions of LPI for different PGAs and M6.9 earthquake. b. Liquefaction probabilities for M6.9 earthquake. c. Liquefaction probability curve for a magnitude-scaled PGA.

Effect of Depth to Water Table

Depth to the ground water table is an important consideration for hazard mapping. It can significantly affect LPI values. Depth to the water table for the hazard maps of greater Oakland was incorporated directly into the complementary cumulative frequency distributions of LPI. Ground water in the Oakland area is not developed and the water table is stable except for a seasonal fluctuation. LPI values for each sounding were computed with the water-table depth at the location of the sounding. These values were then used to compute the complementary cumulative frequency distributions. In general, this approach requires that the water-table surface be carefully mapped. During the CPT field exploration, depth to the water table was measured if possible at each sounding after the cone was withdrawn. These measurements were then combined with water tables measured in commercial borings to generate a map with hydrologically reasonable gradients.

Where water tables undergo large secular or seasonal fluctuations, selection of the water table for a scenario requires careful consideration. Options for scenario hazard maps include using the extreme (maximum and minimum) depths, historical shallowest depth, and mean depth to water table. The historical shallowest water table may be appropriate for basins where water levels have been lowered by pumping, but may return to natural levels. Figs. 8 and 9 illustrate the impact of water-table depth on LPI and liquefaction hazard. Fig. 8 shows the variation of LPI with depth for different types of surficial geology. Fig. 9 compares the resulting hazard for two water-table scenarios for the northern Santa Clara Valley, California.

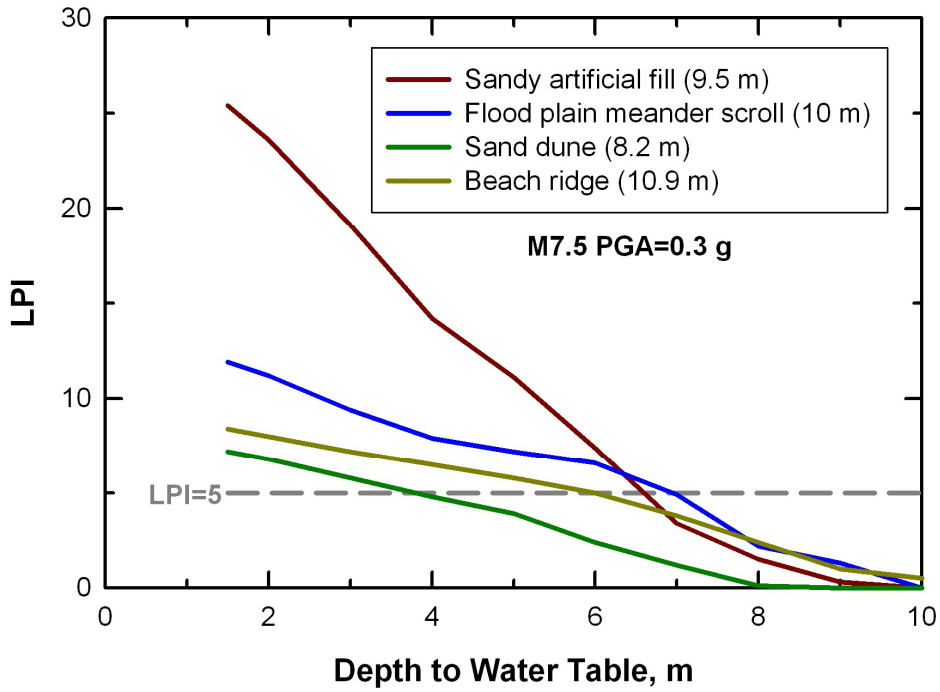

FIG. 8. LPI as a function of depth to water table for four CPT soundings completed in different Holocene geologic units. Values are based on a M7.5 earthquake and PGA=0.3 g. Unit thickness is shown in parentheses in legend.

Fig. 8 illustrates the effect on LPI of depth to the water table for individual CPT soundings completed in four different surficial geologic units: sandy artificial fill, flood plain meander scroll deposit, sand dune, and beach ridge. The unit penetrated by each sounding was approximately 10 m thick, mostly susceptible to liquefaction, and Holocene in age. Values were computed for each sounding for a M7.5 earthquake with PGA=0.3 g. LPI decreases with increasing depth to the water table for all four units, decreasing to less than five at depths ranging from 4 m for the sand dune deposit to 7 m for the meander scroll deposit. In a deposit with approximately constant *FS*, the slope of the curve of LPI versus water table is a function of *FS*, being higher for units with lower *FS*. The thickness of liquefiable sediment only affects the absolute value of LPI.

Fig. 9 illustrates the accommodation of a temporally variable water table into liquefaction hazard mapping of the northern Santa Clara Valley, California for a M7.8 earthquake on the nearby San Andreas Fault. The fault extends far outside of the study area. Two alternative water-table scenarios were considered. Ground-water levels, particularly in the confined aquifer beneath the valley, are subject to large fluctuations because ground water is managed and heavily pumped. The water table in the shallow unconfined aquifer also undergoes water-level fluctuations because of the Mediterranean climate and anthropogenic modifications of the hydrogeologic regime. Two different water-table depth scenarios–1.5 m and 5 m–were assumed in order to capture the approximate temporal extremes of the hazard in the central part of the valley where the hazard is greatest. The 1.5-m depth corresponds approximately to the historical high water level reported in the central part of the study area. These levels still recur during years of high rainfall. The 5-m depth corresponds approximately to the seasonal low in the central part of the area. Probabilities were estimated for both water-table depths. Hazard in the area with the 1.5-m-deep water table (see Fig. 9a) significantly decreases if the water table is at 5 m (see Fig. 9b).

Spatial Homogeneity of Surficial Geologic Units

Groupings of soundings to compute complementary cumulative frequency distributions are an important consideration in the approach by Holzer et al. (2002; 2006a). Grouping by surficial geologic unit assumes that each unit is approximately spatially homogeneous from a liquefaction hazard perspective. Common practice when mapping surficial geologic units is to use criteria based on geomorphologic expression and agricultural soil type, and not based on geotechnical properties. Groupings can be evaluated by comparing liquefaction probability curves for different surficial geologic units (Fig. 10). Comparison of the data in Fig. 10 for Holocene alluvial fan deposits in the northern Santa Clara Valley (Fig. 11) indicates that Qhly (young Holocene levee deposits) has a significantly higher hazard than do the other units, Qhf/Qhfy, Qhff, and Qhl. In fact, the other fan deposits are indistinguishable from a liquefaction hazard perspective and can be fit adequately with a single curve. The comparison suggests that all of the facies in the Holocene

alluvial fan deposits except for Qhly can be treated as a single unit from a liquefaction hazard perspective.

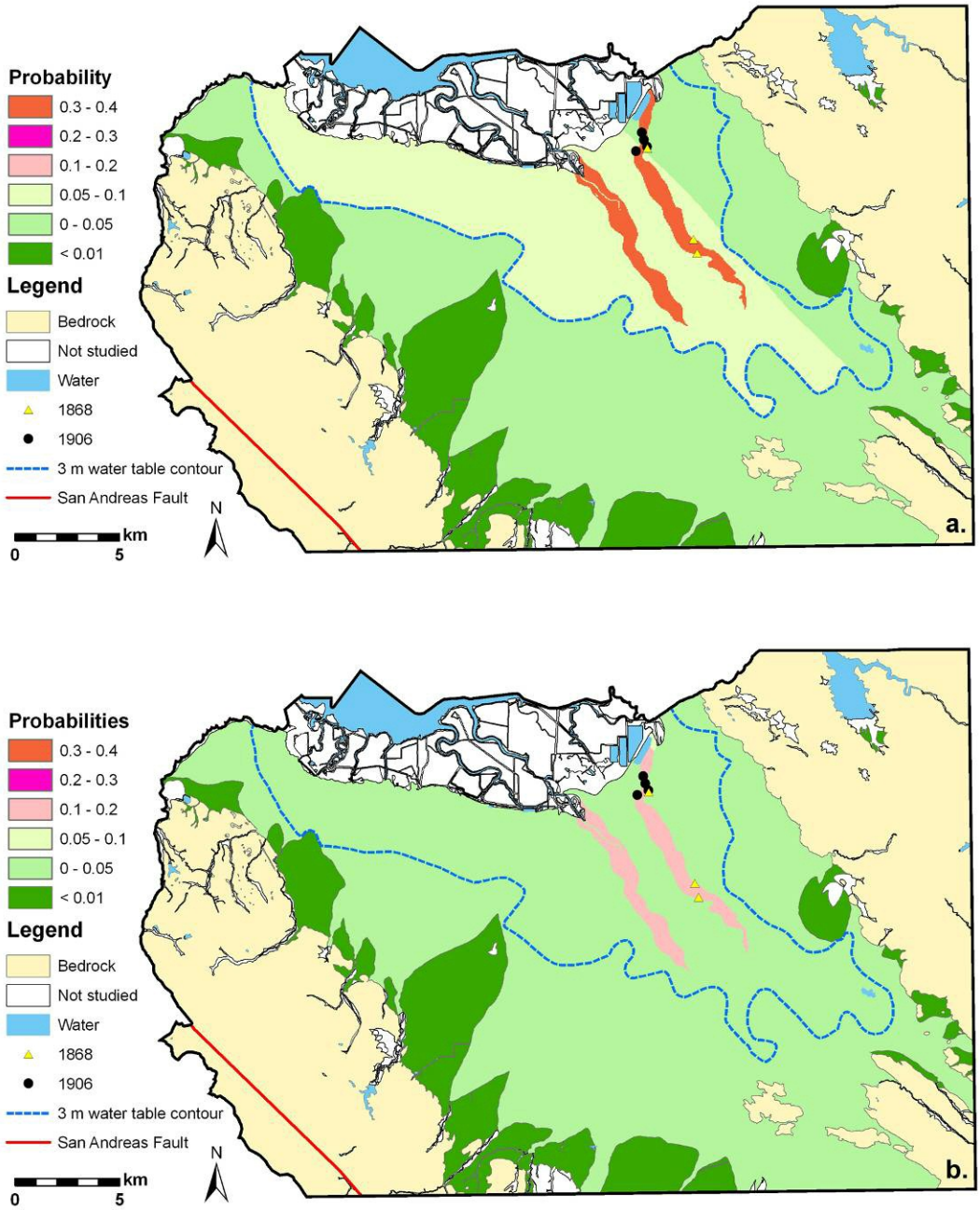

FIG. 9. Probability of liquefaction in the northern Santa Clara Valley, California, for a M7.8 earthquake on the San Andreas Fault. The area is at the south end of San Francisco Bay. a. Assumed water-table depth is 1.5 m in the central part of the valley (outlined in blue). Water-table depth is 5 m elsewhere. b. Assumed water-table depth is 5 m.

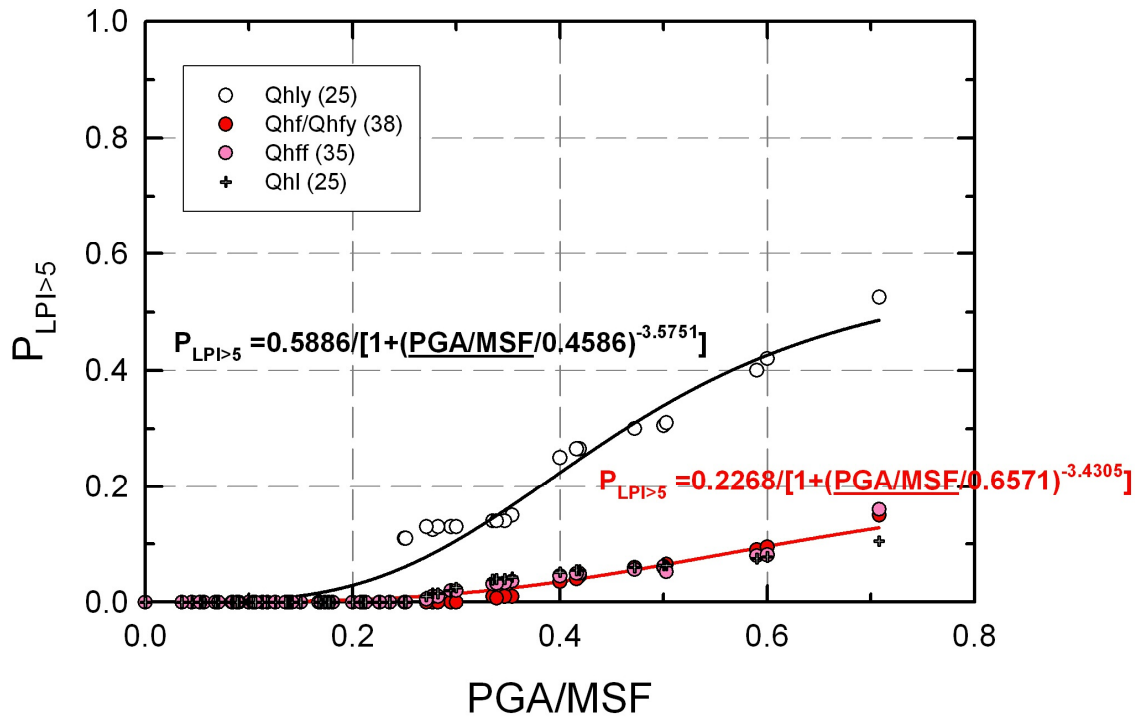

FIG. 10 Liquefaction probability curves for Holocene alluvial fan deposits in the northern Santa Clara Valley, California. Number of soundings in each deposit is shown in parentheses. Water table depth is 5 m.

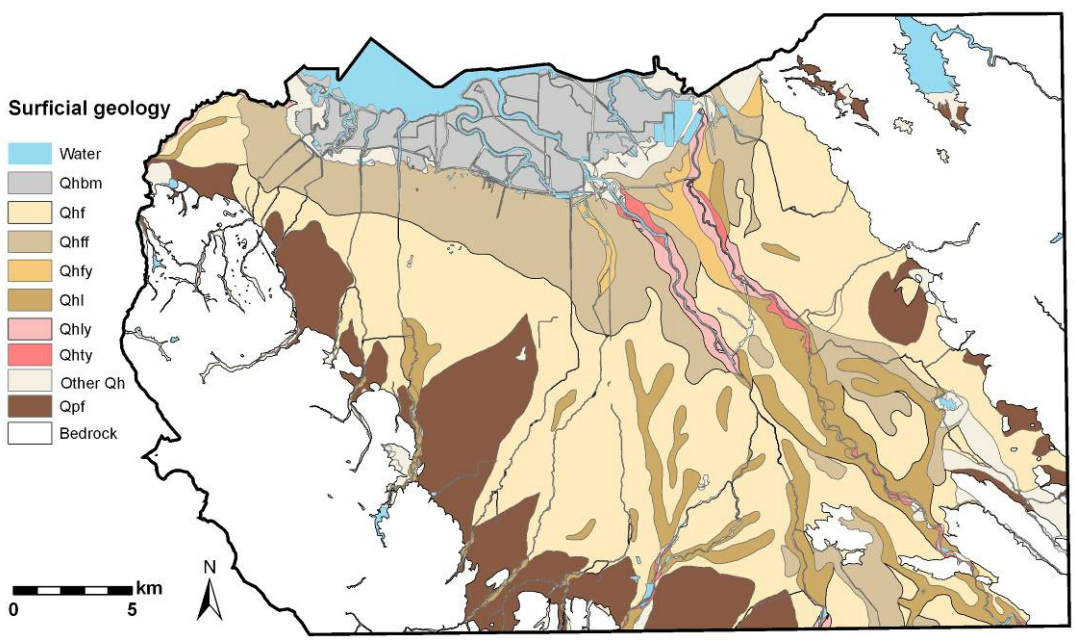

FIG. 11. Map of surficial geology of northern Santa Clara Valley, California (Simplified from Witter et al., 2006). Qh and Qp, respectively, are Holocene and Pleistocene units.

Geologic considerations also may provide useful insight for groupings. In the greater Oakland area, mapped Holocene alluvial fan facies could not be distinguished at depth with CPT soundings, which is consistent with the depositional framework of the alluvial-fan environment. The Holocene alluvial fan was an active depositional surface until urbanization and channelization of streams began late in the 19th century. Such fans aggrade as streams migrate laterally across the surface of the fan. Thus, the modern patterns of sedimentary deposition, which are what is being geologically mapped, should not be expected to extend to depth, particularly along the transverse axes of the fans. Because Holocene fan facies could not be distinguished from a geotechnical perspective, they were grouped together to produce a single complementary cumulative frequency distribution of LPI.

Conversely, a mapped surficial unit may be spatially inhomogeneous from a geotechnical perspective despite being mapped as a single surficial unit by geologists. For example, subsurface exploration by CPT of the Merritt Sand revealed that the formation had significantly higher liquefaction potential in the western part of its outcrop area in Oakland than elsewhere. Holzer et al. (2006a) inferred that that the western part had a different geologic stratigraphy and history and they recognized it as a separate geotechnical unit based on its liquefaction potential.

Finally, thickness of a mapped unit can be important when using surficial geologic maps to delineate liquefaction hazard. Where a unit (or part of it) is thin and above the water table, the liquefaction hazard derives from underlying units that are below the water table and not from the mapped surficial unit. With the Oakland map for example, the area where Holocene alluvial fan deposits were above the water table was delineated using the water-table map, and the liquefaction hazard determined for the underlying Pleistocene alluvial fan deposits was assigned to this area (Holzer et al., 2006a).

Mapping Severity of Liquefaction

Most LPI-based liquefaction hazard maps predict areas of potential liquefaction, not the severity of the ground deformation. Toprak and Holzer (2003) proposed that the intensity of ground deformation generally increases with LPI, and that a threshold LPI≥12 corresponds to the onset of lateral spreading. Fig. 12 is a map of the Santa Clara Valley that uses this threshold to estimate the probability of lateral spreading. The map was prepared with the same procedure as that used to produce the map in Fig. 9, but by using the higher LPI threshold, the probability applies to lateral spreading. The reliability of lateral spread hazard maps based solely on LPI remains to be demonstrated. Although some correlation between ground deformation and LPI is to be expected, lateral spreading also is influenced by factors not included in LPI, such as local static shear stress, continuity of liquefiable layers, and whether or not the soil is contractive.

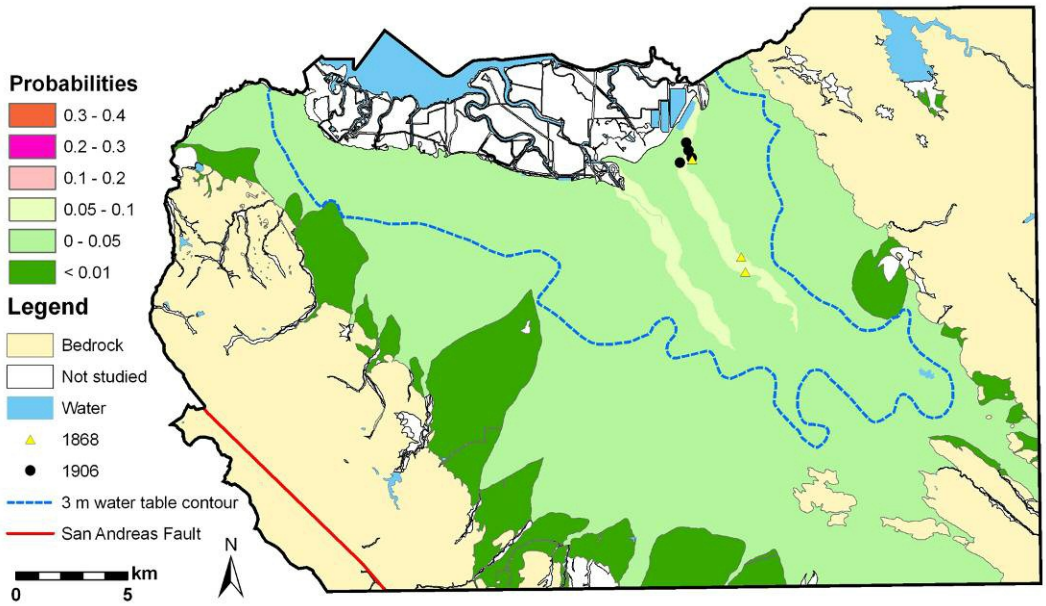

FIG. 12. Probability of liquefaction-induced lateral spreading in the northern Santa Clara Valley, California, for a M7.8 earthquake on the San Andreas Fault. Water table conditions are same as those used to produce liquefaction map in Fig. 8a.

Evaluations of Probabilistic Scenario Maps

The ultimate test of a mapping methodology is the accuracy of its predictions. At this early phase of the development of probabilistic liquefaction hazard maps, probabilistic scenario maps are particularly useful because predictions can be evaluated either with historical events or after future earthquakes that approximate the proposed scenario.

The percent area that is predicted to show evidence of liquefaction in the greater Oakland area is consistent with experience in recent earthquakes where similar geologic deposits have been subjected to near-field ground motion. For example, the ~73% of the area underlain by artificial fill that is predicted to liquefy is consistent with the extensive liquefaction of loose fills during the 1995 earthquake in Kobe, Japan (Hamada et al., 1995). Similarly, the ~3% of the area underlain by Holocene alluvial fan deposits that is predicted to liquefy is consistent with field observations following the 1994 Northridge, California, M6.7 earthquake, where a small area underlain by the alluvial fan deposits liquefied in the epicentral area in the San Fernando Valley (Holzer et al., 1999). One, albeit modest, test of the predictive capability of the methodology used for the Oakland map is the liquefaction performance of sandy artificial fill during the 1989 Loma Prieta (M6.9) earthquake. Based on maps of liquefaction caused by the earthquake (Tinsley et al., 1998), approximately 14% of the area underlain by artificial fill liquefied. Complementary cumulative frequency distributions of LPI for a Loma Prieta earthquake scenario predict that 13% of the fill should have liquefied (Holzer et al., 2006c). Fig. 13

compares locations of liquefaction caused by the 1989 Loma Prieta earthquake with predicted liquefaction probabilities. Liquefaction in general occurred in areas of higher probability (>0.1).

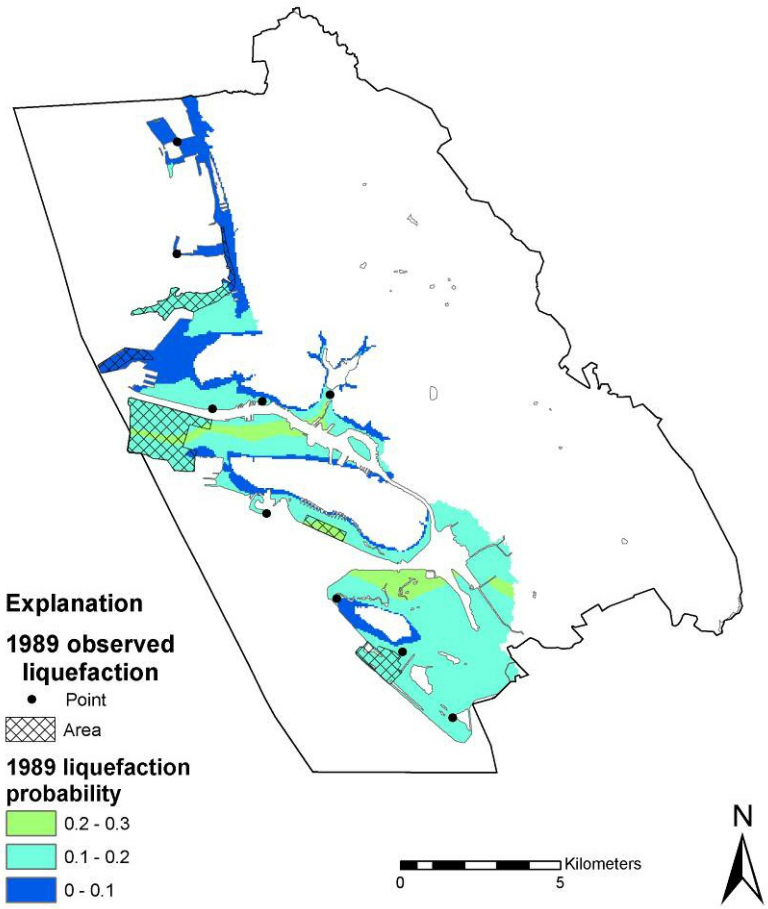

FIG. 13. Comparison of predicted liquefaction probabilities for the 1989 M6.9 Loma Prieta earthquake and locations of observed liquefaction in sandy artificial fills along eastern margin of San Francisco Bay, near Oakland, California. (Holzer et al., 2006c, Fig. 10).

Liquefaction predicted by the hazard map for northern Santa Clara Valley can be evaluated to a limited extent with observations from large historical earthquakes. The valley was strongly shaken by the 1868 M~6.7 Hayward Fault and 1906 M7.8 San Andreas Fault earthquakes. Lawson (1908) and Youd and Hoose (1978) described multiple occurrences of liquefaction during these earthquakes. Reports of liquefaction were limited to the flood plain of Coyote Creek, the easternmost of the two high (probability>0.3) hazard areas (Fig. 9a). Many of the descriptions suggested lateral spreading. However, a systematic exploration for these effects was not conducted following each earthquake.

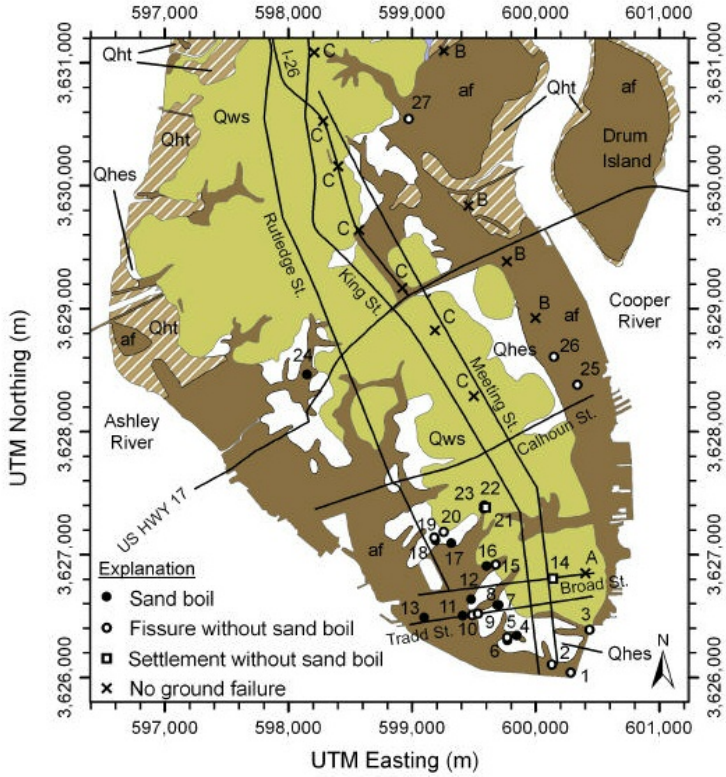

FIG. 14. Geologic map of Charleston peninsula, South Carolina, by Weems and Lemon, 1993), with locations of 1886 liquefaction and ground deformation (Hayati and Andrus, 2007, Fig. 2). [af is artificial fill; Qht are Holocene tidal marsh deposits; Qhes are Pleistocene barrier island deposits; and Qws are barrier sand facies of the Pleistocene Wando Formation.]

The liquefaction hazard map of the Charleston peninsula (Fig. 5) by Juang and Li (2007) can be evaluated with locations of liquefaction in 1886 (Fig. 14). Although liquefaction was extensive at the southern tip of the Charleston peninsula in their area of high hazard, it is not extensive in their high hazard area in the northern part of the peninsula. The high hazard zone at the tip of the peninsula is based on a single CPT sounding. Locations of historical liquefaction in Charleston appear to be better predicted by the hazard map prepared by Hayati and Andrus (2007) (Fig. 15). They computed median LPI values for surficial geologic units and applied the Iwasaki scale to classify hazard areas.

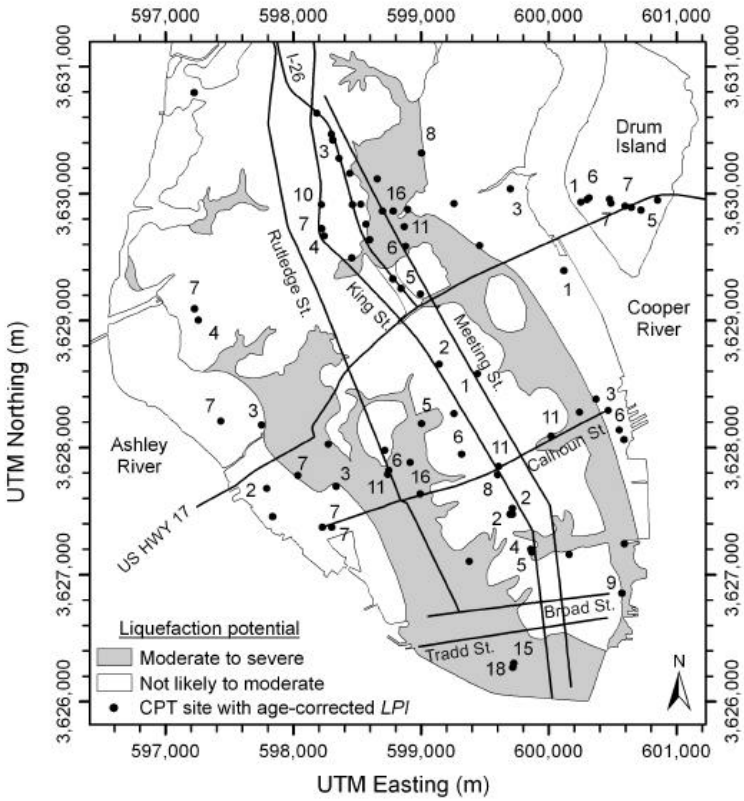

FIG. 15. Liquefaction hazard map of the Charleston peninsula, South Carolina, by Hayati and Andrus (2007, Fig. 7).

PROBABILISTIC LIQUEFACTION HAZARD EVALUATIONS AND MAPPING

Probabilistic liquefaction hazard analysis is just an extension of the PSHA methodology that was developed by Cornell (1968). In fact, to paraphrase McGuire (2004), a PLHA map should simply be viewed as a process by which probabilistic results are computed and documented. A reasonable goal of regional mapping of probabilistic liquefaction hazard is to predict the spatial distribution of the probability of liquefaction for a given return period.

In recent years the trend in engineering practice to apply probabilistic criteria to seismic design has prompted several efforts to characterize liquefaction hazard at specific sites in a probabilistic framework. Typically these efforts have predicted annual probabilities of liquefaction based on blow counts in critical susceptible layers. These efforts have sought neither to predict probabilities of the consequences of the liquefaction of a layer nor to map liquefaction hazard on a regional basis. Their focus has been on site specific investigations. These efforts might be more appropriately called probabilistic hazard liquefaction evaluations.

The first probabilistic hazard liquefaction evaluation of which the author is aware was by Yegian and Whitman (1978). They predicted the annual probability of liquefaction for a specific site condition based on a theoretical relation between

earthquake magnitude and maximum distance to liquefaction. Atkinson et al. (1984) combined a deterministic version of the Seed-Idriss simplified procedure (Seed and Idriss, 1982) and Cornell's (1968) PSHA to predict annual probability of liquefaction as a function of SPT blow count. Marrone et al. (2003) were the first to incorporate probabilistic versions of the simplified procedure into a PSHA-type liquefaction analysis. They estimated annual probabilities of liquefaction at specific sites of engineering interest. Kramer and Mayfield (2007) performed a similar analysis and applied the probabilistic update by Cetin et al. (2004) to the simplified procedure to predict the return period of liquefaction for generic site conditions.

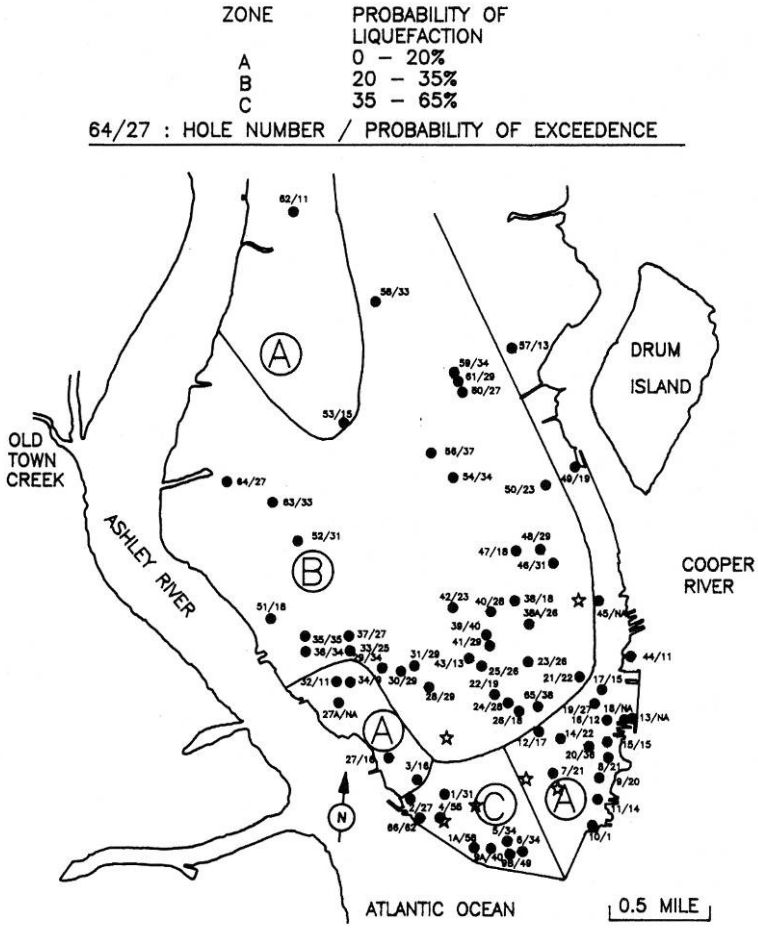

FIG. 16. Liquefaction probability of exceedance in 50 years for the Charleston peninsula, South Carolina. Stars show locations of liquefaction in 1886. (Elton and Hadj-Hamou (1990, Fig. 6).

Youd and Perkins (1978) were the first to apply PSHA concepts to regional mapping of liquefaction hazard. They outlined a procedure that combined a map of "ground failure susceptibility" of geologic units with a map of "ground failure opportunity" to produce a map of "ground failure potential." Ground failure opportunity was based on an empirical relation between earthquake magnitude and the maximum distance to liquefaction. Combining the magnitude-distance relation

with a Poisson earthquake source model, they circumscribed areas with different return periods within which local liquefaction could be expected. A formal procedure to combine the maps was stymied, however, by the absence of a quantitative characterization of liquefaction susceptibility. Thus, the map of "ground failure potential" consisted of two overlaid maps: (1) a ground failure susceptibility map that showed relative liquefaction susceptibility of deposits, and (2) a ground failure opportunity map that delineated areas of potential liquefaction with different return periods (Youd and Perkins, 1978, Fig. 7).

Elton and Hadj-Hamou (1990) used SPT penetration resistance to estimate ground failure potential on the Charleston peninsula, South Carolina. They identified and characterized the susceptibility of liquefiable layers with SPT blow counts in more than 200 soil borings. The layers were portrayed in 71 composite borings, and the variability of the blow counts was used to estimate the uncertainty of the liquefaction susceptibility of the layer. The liquefaction probability at each composite boring was determined by the layer with the highest probability. The liquefaction probability was defined as the probability of exceedance in 50 years of the critical PGA, which is the PGA required to cause $FS<1$ in the layer. They subdivided the peninsula into three zones on the basis of their range of probabilities (Fig. 16). Adequate surficial geologic maps were not available at the time of the mapping to help delineate the boundaries of the zones, but the zones loosely corresponded to the surficial geology as subsequently mapped by Weems and Lemon (1993) shown in Fig. 14. The map implies only the most susceptible layer liquefied. It does not predict the consequences of the liquefaction of the layer.

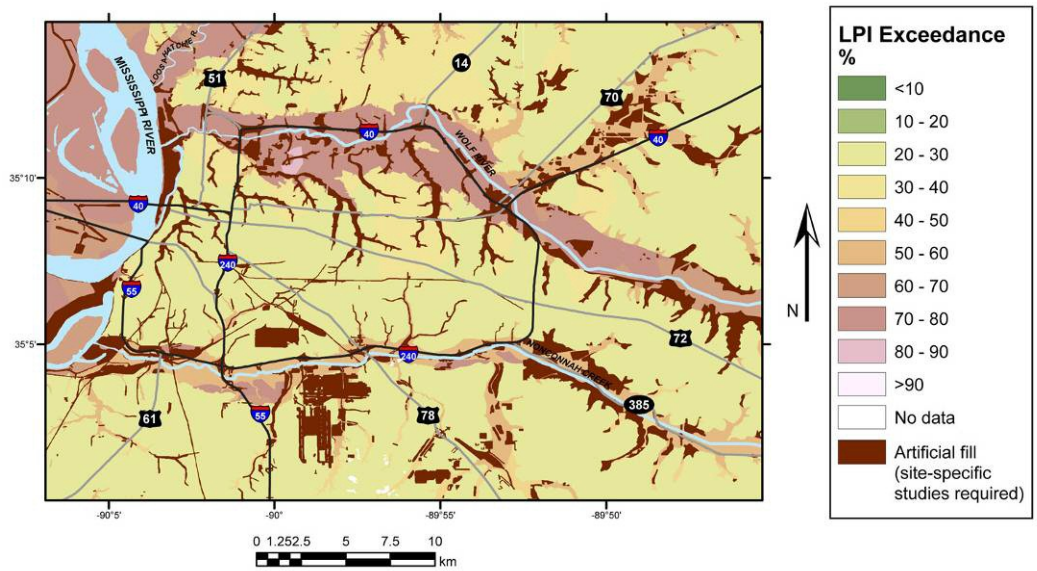

FIG. 17. Probabilistic liquefaction hazard map of Memphis, Tennessee showing 5% probability of exceedance in 50 years of LPI>5. (Cramer et al., 2008, Fig. 6b)

Cramer et al. (2008) were the first to use LPI in a formal PLHA to produce probabilistic liquefaction hazard maps. Their maps of Memphis, Tennessee, predicted probabilities of exceeding LPI values of 5 and 15. These are the thresholds, respectively at which severe liquefaction is unlikely and likely with the Iwasaki scale.

They produced maps for 10%, 5%, and 2% probabilities of exceedance in 50 years, i.e., return periods of 495, 975, 2475 years, respectively. The maps were developed from probabilistic ground motions and earthquake magnitudes from the USGS national seismic hazard model (Frankel et al., 2002). Liquefaction potential was estimated with liquefaction probability curves developed by Rix and Romero-Hudock (2007) for surficial geologic units in Memphis. Cramer et al. (2008) included the effect of site response on ground motion. Their liquefaction hazard map with a 5% probability of exceedance in 50 years of LPI>5 (Fig. 17) predicts a hazard that is comparable to the hazard in the probabilistic liquefaction scenario map by Rix and Romero-Hudock (2007) for a M7.7 earthquake in the southern New Madrid seismic zone. Ground motions for the M7.7 earthquake and the probabilistic PGA map with a 5% probability of exceedance in 50 years are similar.

DISCUSSION

LPI has become a popular parameter for regional mapping of both liquefaction potential and probability of liquefaction. Its advantage for mapping over the simplified procedure is that it predicts the liquefaction performance of the entire soil column, not just a soil element or layer. This is a significant advantage because, as a spatial parameter, LPI can be used to predict the spatial pattern of liquefaction, not just the liquefaction of layers. LPI also can enable usage of surficial geologic maps to expedite regional liquefaction hazard mapping.

Two approaches that rely on LPI have been developed for probabilistic mapping of liquefaction. The approach by Holzer et al. (2002; 2006a) uses complementary cumulative frequency distributions of LPI to estimate liquefaction probabilities of spatially homogeneous surficial geologic units. By applying threshold values at which either liquefaction or lateral spreading is expected, the conditional probability of liquefaction (or lateral spreading) given an earthquake magnitude and PGA can be estimated. Both probabilistic liquefaction scenario maps and PSHA-based liquefaction hazard maps have been produced with this approach. The approach by Juang and Li (2007) relies directly on the spatial pattern of LPI values to estimate liquefaction probabilities. Both approaches rely on versions of the Seed-Idriss simplified procedure to compute LPI.

The ultimate test of these approaches is how well maps based on them predict actual liquefaction performance. The predicted performance of deposits in the greater Oakland area and the northern Santa Clara Valley, California, are consistent with both their historical performance and the performance of similar geologic deposits in other earthquakes. The tests are modest, however. Comparison of predictions with observations from 1886 for the Charleston peninsula by Juang and Li (2007) is less clear, but predicted probabilities appear to be high.

The dependency of LPI on the simplified procedure raises several issues. On the one hand the dependency is an advantage in that LPI relies on a well established geotechnical methodology to analyze liquefaction potential. On the other hand it is a disadvantage in that the simplified procedure continues to evolve. Probabilistic versions of the simplified procedure introduce another complication. While these probabilistic versions reflect the growing demand in engineering design for probabilistic evaluations of risk, they require a modification of the original definition

of LPI, which is based on factor of safety. Lee et al. (2003) attempted such a redefinition of LPI, but found it produced an LPI scale that differed significantly than those by Iwasaki et al. (1982) and Toprak and Holzer (2003). As was discussed, this prompted them to rename their index parameter. Nevertheless, probabilistic versions of the simplified procedure have the advantage of reconciling fundamental differences in the statistical significance of factors of safety determined by CPT and SPT-based deterministic boundary curves. For example, Toprak et al. (1999) associated the SPT- and CPT-based deterministic boundary curves recommended by Youd et al. (2001) with probabilities of liquefaction triggering of 20% (for blow counts less than 10) and 50%, respectively.

There is a need for caution when different versions of the simplified procedure are used to calibrate LPI than are used to map with LPI. Although some investigators have been consistent in using the same version of the simplified procedure for both calibration and mapping, others have not. Maps that rely on the calibration by Iwasaki et al. (1982) but rely on another version for mapping are challenging to evaluate. As indicated by Fig. 1, the factor of safety computed by the "simple analysis" of Iwasaki et al. (1982) may differ substantially from that by the Seed-Idriss simplified procedure. Some investigators have addressed the impact of different versions of the Seed-Idriss simplified procedure by comparing predictions with different versions. Sensitivity tests by Kayabili and West (1994), Cresellani et al. (1999), and Lee et al. (2003) indicated the impact of different versions on mapping was minor.

The reliability of the simplified procedure for evaluation of the liquefaction potential of pre-Holocene geologic deposits is particularly important for liquefaction hazard mapping. Older Holocene and Pleistocene surficial geologic deposits typically must be evaluated in regional mapping efforts. The simplified procedure is based on case histories that include only Holocene deposits. It is not known how well the procedure evaluates the liquefaction potential of Pleistocene deposits, which typically have undergone more diagenesis and earthquake shaking than Holocene deposits. Some investigators (e.g., Leon et al., 2006) have proposed age corrections when applying the simplified procedure to these older deposits.

LPI also has some inherent shortcomings when it is applied to regional mapping. The reliance on complementary cumulative frequency distributions of LPI requires a large number of soundings or borings in geologic deposits with low liquefaction potential. For example, a deposit with a liquefaction probability of 10% can be characterized with a small number (<30) of borings or soundings. As the probability decreases, the number of exploratory soundings or borings required to document the liquefaction potential of the surficial unit increases. LPI is not an efficient tool for mapping in these types of deposits if the purpose is to distinguish differences between deposits with low liquefaction potential. LPI also is not a reliable predictor of the performance of soils in which the liquefaction hazard derives from thin but continuous liquefiable layers. Such soils will have low LPI, which suggest a low hazard, but the continuity of the layers may provide conditions conducive to lateral spreading. The Balboa Boulevard lateral spread, which failed during the 1994 Northridge, California, earthquake in a thin liquefied interval, is an example of this condition (Holzer et al., 1999).

Although probabilistic mapping of liquefaction hazard may meet the demand by engineers for performance-based design, it can obscure nonprobabilistic insights from surficial geologic mapping that can further resolve liquefaction hazard. For example, Holzer and Bennett (2007) documented how specific geologic conditions determined the boundaries of many lateral spreads. These boundaries are where ground strains are largest. Locations of lateral spreads and their boundaries may be more deterministic than a probabilistic map might imply.

ACKNOWLEDGMENTS

The author thanks Chris H. Cramer and T. Leslie Youd for constructive reviews of the manuscript. Thomas E. Noce drafted Figs. 9, 11, and 12. The author also thanks Ronald D. Andrus and John C. Tinsley, III, for comments on parts of the manuscript. The author is indebted to Michael J. Bennett, Thomas E. Noce, and Selcuk Toprak for their collaborative exploration of LPI. The PG&E-USGS CRADA and Nuclear Regulatory Commission supported parts of this research.

REFERENCES

Atkinson, G.M., Finn, W.D.L., and Charlwood, R.G. (1984). "Simple computation of liquefaction probability for seismic hazard applications." *Earthquake Spectra* 1(1): 107-123.

Baise, L.G., Higgins, R.B., and Brankman, C.M. (2006). "Liquefaction hazard mapping-Statistical and spatial characterization of susceptible units." *J. Geotechnical and Geoenvironmental Engrg.* 132(6): 705-715.

BSSC (2001). "2000 Edition NEHRP recommended provisions for seismic regulations for new buildings and other structures," FEMA 368, Part 1 (provisions), Federal Emergency Management Agency, Washington, D.C.

Cetin, K.O., Seed, R.B., Kiureghian, A.D., Tokimatsu, K., Harder, L.F., Kayen, R.E., and Moss, R.E.S. (2004). "Standard penetration test-based probabilistic and deterministic assessment of seismic soil liquefaction potential." *J. Geotechnical and Geoenvironmental Engrg.* 130(12): 1314-1340.

Cornell, C.A. (1968). "Engineering seismic risk analysis." *Seismological Society of America Bull.* 58(5): 1583-1606.

Cramer, C.H., Rix, G.J., and Tucker, K. (2008). "Probabilistic liquefaction hazard maps for Memphis, Tennessee." *Seismological Research Letters* 78 (in press).

Crespanelli, T., Madiai, C., and Vannucchi, G. (1999). "Zoning for liquefaction risk in an Italian coastal town using CPT." *Earthquake Geotech. Engrg.*, A.A. Balkema, Rotterdam: 561-566.

Divakarla, P.K., Hoyos, L.R., Jr., and Macari, E.J. (1998). "Assessment of liquefaction potential of western Puerto Rico." *Proc. 3rd Geotechnical Earthquake Engrg. and Soil Dynamics Conference*. ASCE/Reston: 530-541.

Elton, D.J., and Hadj-Hamou, T. (1990). "Liquefaction potential map for Charleston, South Carolina." *J. Geotechnical Engrg.* 116(2): 244-265.

Frankel, A., Petersen, M., Mueller, C., Haller, K., Wheeler, R., Leyendecker, E., Wesson, R., Harmsen, S., Cramer, C., Perkins, D., and Rukstales, K. (2002).

"Documentation for the 2002 update of the national seismic hazard maps." *Open-file Report 02-420*, U.S. Geological Survey, Denver, CO.

Frost, J.D., Carroll, D.P., and Rockaway, T.D. (1997). "Spatial liquefaction analysis." *Spatial Analysis in Soil Dynamics and Earthquake Engrg*., GSP No. 67, ASCE, New York/NY: 70-86.

Hamada, M., Isoyama, R., and Wakamatsu, K. (1995). "The 1995 Hyogoken-Nanbu (Kobe) earthquake-Liquefaction, ground displacement, and soil condition in the Hanshin area." The School of Science and Engrg., Waseda University, Tokyo: 194 p.

Hayati, H., and Andrus, R. (2007). "Liquefaction potential map of Charleston, South Carolina, based on the 1886 earthquake." Final report to the U.S. Geological Survey (06HQGR0058).

Helley, E.J., and Graymer, R.W. (1997). "Quaternary geology of Alameda County, and parts of Contra Costa, Santa Clara, San Mateo, San Francisco, Stanislaus, and San Joaquin Counties, California: A digital database." *Open-file Report 97-97*, U.S. Geological Survey, Menlo Park, CA.

Holzer, T.L., and Bennett, M.J. (2007). "Geologic and hydrogeologic controls of boundaries of lateral spreads: Lessons from USGS case histories." *First North American Landslide Conference*, SP No. 23, AEG: 502-522.

Holzer, T.L., Bennett, M.J., Noce, T.E., Padovani, A.C., and Tinsley, J.C., III (2002). "Liquefaction hazard and shaking amplification maps of Alameda, Berkeley, Emeryville, Oakland, and Piedmont: A digital database." *Open-file Report 02-296*, U.S. Geological Survey, Menlo Park, CA.

Holzer, T.L., Bennett, M.J., Noce, T.E., Padovani, A.C., and Tinsley, J.C., III (2006a). "Liquefaction hazard mapping with LPI in the greater Oakland, California, area." *Earthquake Spectra* 22(3): 693-708.

Holzer, T.L., Bennett, M.J., Ponti, D.J., and Tinsley, J.C., III (1999). "Liquefaction and soil failure during the 1994 Northridge earthquake." *J. Geotechnical and Geoenvironmental Engrg.* 125(6): 438-452.

Holzer, T.L., Blair, J.L., Noce, T.E., and Bennett, M.J. (2006b). "LiqueMap: A real-time post earthquake map of liquefaction probability." *Proc. 8th U.S. National Conference on Earthquake Engrg.* (CD-ROM), EERI, Oakland, CA.

Holzer, T.L., Blair, J.L., Noce, T.E., and Bennett, M.J. (2006c). "Predicted liquefaction of East Bay fills during a repeat of the 1906 San Francisco earthquake." *Earthquake Spectra* 22(S2): S261-S278.

Holzer, T.L., Noce, T.E., Bennett, M.J., Tinsley, J.C., III and Rosenberg., L.I. (2005a). "Liquefaction at Oceano, California, during the 2003 San Simeon earthquake." *Seismological Society of America Bull.* 95(6): 2396-2411.

Holzer, T.L., Padovani, A.C., Bennett, M.J., Noce, T.E., and Tinsley, J.C., III (2005b). "Mapping NEHRP V_{S30} site classes." *Earthquake Spectra* 21(2): 353-370.

Hosseini, S.M.M.M. (1998). "Microzonation for liquefaction in Busehr, Iran." *Proc. 11th European Conference on Earthquake Engrg.* (CD-ROM), A.A. Balkema, Rotterdam.

Idriss, I.M., and Boulanger, R.W. (2006). "Semi-empirical procedures for evaluating liquefaction potential during earthquakes." *Soil Dynamics and Earthquake Engrg.* 26(2-4): 115-130.

Iwasaki, T., Tatsuoka, F., Tokida, K.-i., and Yasuda, S. (1978). "A practical method for assessing soil liquefaction potential based on case studies at various sites in Japan." *Proc. 2nd International Conference on Microzonation*: 885-896.

Iwasaki, T., Tokida, K., Tatsuoka, F., Watanabe, S., Yasuda, S., and Sato, H. (1982). "Microzonation for soil liquefaction potential using simplified methods." *Proc. 3rd International Earthquake Microzonation Conference*: 1319-1330.

Juang, C.H., Jiang, T., and Andrus, R.D. (2002). "Assessing probability-based methods for liquefaction potential evaluation." *J. Geotechnical and Geoenvironmental Engrg.* 128(7): 580-589.

Juang, C.H., and Li, D.K. (2007). "Assessment of liquefaction hazards in Charleston quadrangle, South Carolina." *Engrg. Geology* 92(1-2): 59-72.

Juang, C.H., Yuan, H., Lee, D.-H., and Lin, P.-S. (2003). "Simplified cone penetration test-based method for evaluating liquefaction resistance of soils." *J. Geotechnical and Geoenvironmental Engrg.* 129(1): 66-80.

Juang, C.H., Yuan, H., Li, D.K., Yang, S.H., and Christopher, R.A. (2005). "Estimating severity of liquefaction-induced damage near foundation." *Soil Dynamics and Earthquake Engrg*. 25(5): 403-411.

Kayabali, K., and West, T.R. (1994). "Liquefaction susceptibility evaluation for the City of Evansville, Indiana." *Bull. Association Engrg. Geologists* 31(2): 231-253.

Kramer, S.L., and Mayfield, R.T. (2007). "Return period of soil liquefaction." *J. Geotechnical and Geoenvironmental Engrg.* 133(7): 802-813.

Lawson, A.C. (Editor) (1908). "The California Earthquake of April 18, 1906." *Report of the State Earthquake Investigation Commission*. Carnegie Institution of Washington Publication No. 87: 192 p.

Lee, D.-H., Ku, C.-S., and Yuan, H. (2003). "A study of the liquefaction risk potential at Yuanlin, Taiwan." *Engrg. Geology* 71(1-2): 97-117.

Lenz, J.A., and Baise, L.G. (2007). "Spatial variability of liquefaction potential in regional mapping using CPT and SPT data." *Soil Dynamics and Earthquake Engrg.* 27(7): 690-702.

Leon, E., Gassman, S.L., and Talwani, P. (2006). "Accounting for soil aging when assessing liquefaction potential." *J. Geotechnical and Geoenvironmental Engrg.* 132(3): 363-377.

Li, D.K., Juang, C.H., and Andrus, R.D. (2006a). "Estimation of liquefaction effect by means of liquefaction potential index." GSP No. 152. ASCE, Reston/VA: 359-364.

Li, D.K., Juang, C.H., and Andrus, R.D. (2006b). "Liquefaction potential index: a critical assessment using probability concept." *Taiwan Geotechnical Society J. GeoEngrg.* 1(1): 11-24.

Liao, S.S.C., Veneziano, D., and Whitman, R.V. (1988). "Regression models for evaluating liquefaction probability." *J. Geotechnical Engrg.* 114(4): 389-411.

Luna, R., and Frost, D.J. (1998). "Spatial liquefaction analysis system." *J. Computing in Civil Engrg.* 12(1): 48-56.

Mabey, M.A., Madin, I.P., Youd, T.L., and Jones, C.F. (1993). "Earthquake hazards of the Portland quadrangle, Multnomah and Washington Counties, Oregon, and Clark County, Washington." *Geological Map Series GMS-79*, Oregon Department of Geology and Mineral Industries, Portland, OR.

Marrone, J., Ostadan, F., Youngs, R., and Litehiser, J. (2003). "Probabilistic liquefaction hazard evaluation: Method and application." *Proc. 17th International Conference on Structural Mechanics in Reactor Technology* (CD-ROM).

McGuire, R.K. (2004). "Seismic hazard and risk analysis." *Monograph 10*, EERI, Oakland, CA: 221 p.

Moss, R.E.S., Seed, R.B., Kayen, R.E., Stewart, J.P., Kiureghian, A.D., and Cetin, K. (2006). "CPT-based probabilistic and deterministic assessment of in situ seismic soil liquefaction potential." *J. Geotechnical and Geoenvironmental Engrg.* 132(8): 1032-1051.

Olsen, M.J., Bartlett, S.F., and Solomon, B.J. (2007). "Lateral spread hazard mapping of the Northern Salt Lake Valley, Utah, for a M7.0 earthquake." *Earthquake Spectra* 23(1): 95-114.

Papathanassiou, G., Pavlides, S., and Ganas, A. (2005). "The 2003 Lefkada earthquake: Field observations and preliminary microzonation map based on liquefaction potential index for the town of Lefkada." *Engrg. Geology* 82(1): 12-31.

Porter, K., Kennedy, R., and Bachmann, R. (2007). "Creating fragility functions for performance-based earthquake engineering." *Earthquake Spectra* 23(2): 471-489.

Power, M.S., and Holzer, T.L. (1996). "Liquefaction maps." *TechBrief 1*, Applied Technology Council, Redwood City, CA: 12 p.

Rix, G.J., and Romero-Hudock, S. (2007). Liquefaction potential mapping in Memphis and Shelby County, Tennessee. Report to U.S. Geological Survey, http:/earthquake.usgs.gov/ regional/ceus/products/download/Memphis_LPI.pdf: 27 p.

Robertson, P.K., and Wride (Fear), C.E. (1998). "Evaluating cyclic liquefaction potential using the cone penetration test." *Canadian Geotech. J.* 35(3): 442-459.

Seed, H.B., and Idriss, I.M. (1971). "Simplified procedure for evaluating soil liquefaction potential." *J. Soil Mechanics and Foundation Engrg.* 97(9): 1249-1273.

Seed, H.B., and Idriss, I.M. (1982). "Ground motions and soil liquefaction during earthquakes." *Monograph 5*. EERI, Oakland, CA: 134 p.

Seed, H.B., Tokimatsu, K., Harder, L.F., and Chung, R.M. (1985). "Influence of SPT procedures in soil liquefaction resistance evaluations." *J. Geotechnical Engrg.* 111(12): 1425-1445.

Sonmez, H. (2003). "Modification of the liquefaction potential index and liquefaction susceptibility mapping for a liquefaction-prone area (Inegol, Turkey)." *Environmental Geology* 44(7): 862-871.

Sonmez, H., and Gokceoglu, C. (2005). "A liquefaction severity index suggested for engineering practice." *Environmental Geology* 48(1): 81-91.

Tinsley, J.C., III, Egan, J.A., Kayen, R.E., Bennett, M.J., Kropp, A., and Holzer, T.L. (1998). "Appendix: Maps and descriptions of liquefaction and associated effects." *The Loma Prieta, California, earthquake of October 17, 1989-Liquefaction.* Professional Paper 1551-B, U.S. Geological Survey, Menlo Park, CA: B287-B314.

Tinsley, J.C., Youd, T.L., Perkins, D.M., and Chen, A.T.F. (1985). "Evaluating liquefaction potential." *Evaluating earthquake hazards in the Los Angeles region-an earth science perspective*. Professional Paper 1360, U.S. Geological Survey, Menlo Park, CA: 263-315.

Toprak, S., and Holzer, T.L. (2003). "Liquefaction potential index: Field assessment." *J. Geotechnical and Geoenvironmental Engrg.* 129(4): 315-322.

Toprak, S., Holzer, T.L., Bennett, M.J., and Tinsley, J.C., III (1999). "CPT- and SPT-based probabilistic assessments of liquefaction potential." *Proc. 7th U.S.-Japan Workshop on Earthquake Resistant Design of Lifeline Facilities and Countermeasures Against Liquefaction*. Multidisciplinary Center for Earthquake Engrg. Technical Report MCEER-99-0019: 69-86.

Ulusay, R., and Kuru, T. (2004). "1998 Adana-Ceyhan (Turkey) earthquake and a preliminary microzonation based on liquefaction potential for Ceyhan Town." *Natural Hazards* 32(1): 59-88.

Weems, R.E., and Lemon, E.M., Jr. (1993). "Geology of the Cainhoy, Charleston, Fort Moultrie, and North Charleston Quadrangles, Charleston and Berkeley Counties, South Carolina." *Miscellaneous Investigation Series I-1935*, U.S. Geological Survey, Reston, VA.

Witter, R.C., Knudsen, K.L., Sowers, J.M., Wentworth, C.M., Koehler, R.D., and Randolph, C.E. (2006). "Maps of Quaternary deposits and liquefaction susceptibility in the central San Francisco Bay region, California." *Open-file Report 06-1037*, U.S. Geological Survey, Menlo Park, CA.

Yegian, M.K., and Whitman, R.V. (1978). "Risk analysis for ground failure by liquefaction." *J. Geotechnical Engrg.* 104(GT7): 921-938.

Youd, T.L., Hansen, C.M., and Bartlett, S.F. (2002). "Revised MLR equations for prediction of lateral spread displacement." *J. Geotechnical and Geoenvironmental Engrg.* 128(12): 1007-1017.

Youd, T.L., and Hoose, S.N. (1977). "Liquefaction susceptibility and geologic setting, World Conference on Earthquake Engineering." *Proc. 6th World Conference on Earthquake Engrg.*: 2189-2194.

Youd, T.L., and Hoose, S.N. (1978). "Historic ground failures in Northern California triggered by earthquakes." *Professional Paper 993*, U.S. Geological Survey, Menlo Park, CA, 177 p.

Youd, T.L. , Idriss, I.M., Andrus, R.D., Arango, I., Castro, G., Christian, J.T., Dobry, R., Finn, W.D.L., Harder, L.F., Jr., Hynes, M.E., Ishihara, K., Koester, J.P., Liao, S.S.C., Marcuson, W.F., III, Martin, G.R., Mitchell, J.K., Moriwaki, Y., Power, M.S., Robertson, P.K., Seed, R.B., and Stokoe, K.H., II (2001). "Liquefaction resistance of soils: Summary report from the 1996 NCEER and 1998 NCEER/NSF workshops on evaluation of liquefaction resistance of soils." *J. Geotechnical and Geoenvironmental Engrg*. 127(10): 817-833.

Youd, T.L., and Noble, S.K. (1997). "Liquefaction criteria based on statistical and probabilistic analyses." *Evaluation of liquefaction resistance of soils.* National Center for Earthquake Engrg. Research Technical Report NCEER-97-0022: 201-205.

Youd, T.L., and Perkins, D.M. (1978). "Mapping liquefaction-induced ground failure potential." *J. Geotechnical Engrg.* 104(4): 433-446.

Youd, T.L., and Perkins, D.M. (1987). "Mapping of liquefaction severity index." *J. Geotechnical Engrg.* 113(11): 1374-1392.